## 2.4 Electronic properties of systems with reduced dimensions

(Following J.H. Davies "The Physics of low-dimensional semiconductors", Cambridge University Press, Cambridge, UK (1998), and lecture notes by D.A. Wharam)

**Recap:**
→ *See Introduction (ch. 1.2(ii), Density of states in reduced dimensions: Electrons)*

Consider a system of $N$ non-interacting electrons (fermions with spin $= \pm\frac{1}{2}\hbar$, i.e. each allowed $\vec{k}$-state in the discretized k-space can accommodate up to two electrons). The electronic density for the number $N$ of occupied states in the Fermi sphere at $T = 0\,\mathrm{K}$ up to the Fermi wave-vector $k_F$ is given by:

$$n = \frac{N}{V} = \frac{2\frac{4}{3}\pi k_F^3}{\frac{8\pi^3}{V}V} = \frac{k_F^3}{3\pi^2} \tag{2.49}$$

The **density of states** (DOS) is an important measure of the number of states which are available for occupancy, or more generally at the Fermi energy, for transport processes. By definition,

$$g(\epsilon) = \frac{1}{V}\frac{\partial N}{\partial \epsilon} = \frac{\partial n}{\partial \epsilon} \tag{2.50}$$

The dimensionality plays a significant role when considering the properties of nanostructures, which are invariably systems of reduced dimensionality. The following dependencies of the DOS on the energy are found (with $m$ the effective mass):

**3D:** $g_{3D}(\epsilon) = \frac{\partial n}{\partial \epsilon} = \frac{\sqrt{2\epsilon m^3}}{\pi^2\hbar^3} = c_{3D}\sqrt{\epsilon}$

**2D:** $g_{2D}(\epsilon) = \frac{1}{A}\frac{\partial N}{\partial \epsilon} = \frac{m}{\pi\hbar^2} = c_{2D}$

**1D:** $g_{1D}(\epsilon) = \frac{1}{L}\frac{\partial N}{\partial \epsilon} = \frac{1}{\pi\hbar}\sqrt{\frac{2m}{\epsilon}} = \frac{c_{1D}}{\sqrt{\epsilon}}$

**0D:** $g_{0D}(\epsilon) = \delta(\epsilon)$

Thus the 3D density of states scales with $\sqrt{\epsilon}$, the 2D density of states is constant, the 1D density of states is proportional to $1/\sqrt{\epsilon}$, and the 0D density of states is a series of discrete delta-functions. Note that the existence of excited states (occupation of more than one state) leads to the formation of subbands, see Fig. 2.26.

In general:

- Volume of a $d$-dimensional sphere: $V_d = \gamma_d R^d$ with $\gamma_d$: $\gamma_1 = 2$, $\gamma_2 = \pi$, $\gamma_3 = \frac{4}{3}\pi$
- Number of states in k-space with a wave vector $\leq$ k: $N = \frac{2V_k}{(2\pi)^d}V = \frac{2\gamma_d k^d}{(2\pi)^d}L^d$
- Electron density: $n = N/V = \frac{2\gamma_d k^d}{(2\pi)^d}$
- $\epsilon = \frac{\hbar^2 k^2}{2m}$ thus $k = \frac{1}{\hbar}\sqrt{2m\epsilon}$
- $g(\epsilon) = \frac{\partial n}{\partial \epsilon} = \frac{d\gamma_d (2m)^{d/2}}{(2\pi\hbar)^d}\epsilon^{\frac{d}{2}-1}$

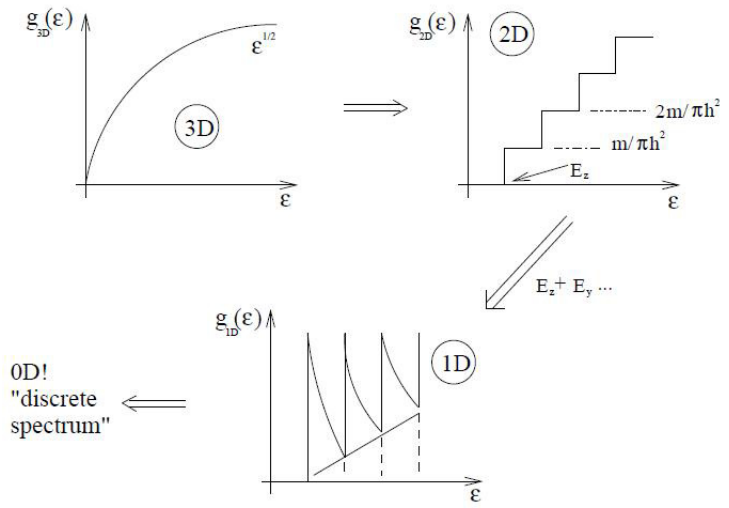


Fig. 2.26: Density of states in 3D, (quasi-)2D, (quasi-)1D and quasi-0D

### 2.4.1 (Quasi-)2dim quantization in heterostructures

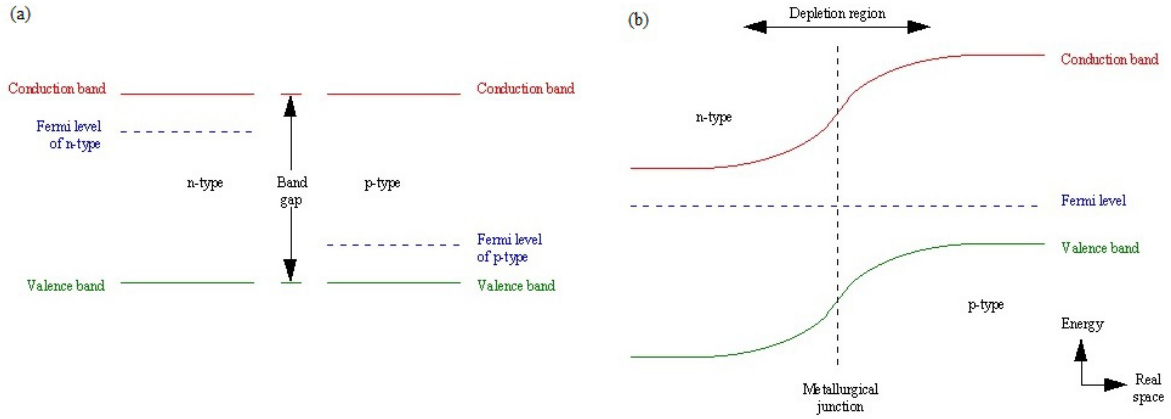


Fig. 2.27: Band structure of the two materials in a homojunction (a) before contact, (b) in contact [ http://www.liv.ac.uk/renewable-energy/about/staff/ken-durose/]

**Homojunction:** Interface between two semiconductors that have identical bandgaps, but may have different properties such as doping (Figure 2.27).

**Heterojunction:** Interface between two semiconductors with different bandgaps.

Semiconductors are characterized by the following energies:
- Band edge energies ($\epsilon_V$ for valence band, $\epsilon_C$ for conductance band)
- Band gap $E_g$
- Chemical potential $\mu$ or Fermi energy $\epsilon_F$
- Electron affinity $\chi$ (surface property)
- Work function $q\Phi_m$ (surface property)

Consider the heterojunction formed between two different bulk semiconductors in contact (Figure 2.28). Bringing the two materials into contact leads to the defini-

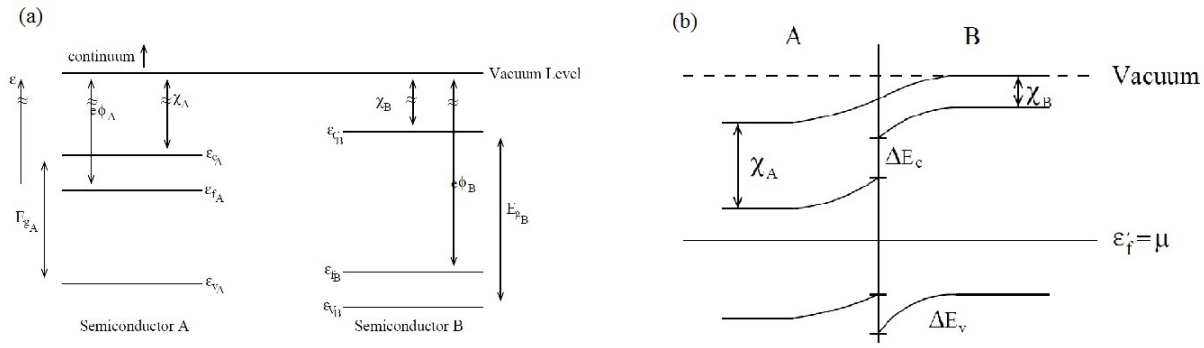


Fig. 2.28: (a) Sample band structure of a heterostructure before contact; (b) positition dependent band bending and band discontinuity in a heterojunction

tion of a well-defined electrochemical potential throughout the whole material, i.e. $\epsilon'_{F_A} = \epsilon'_{F_B} = \mu \; \forall \; \vec{r}$ in the material. As for a standard pn-homojunction, the following effects will occur in the equilibrium state due to a redistribution of charge carriers:
- depletions regions
- band-bending
- creation of a built-in potential $\Phi_{bi}(\vec{r})$.

The resulting position-dependent bandstructure then takes the general form shown in Figure 2.28(b). In contrast to homojunctions, heterojunctions additionally exhibit **band edge discontinuities** ($\Delta\epsilon_C$ and $\Delta\epsilon_V$), which are of crucial significance for device physics and can be influenced by **bandgap engineering**.

*Example:* **Creation of a 2dim electron gas at a heterojunction interface:** Donor doping in a material with a large band gap brought into contact with a neutral (or weakly p-type) material of a smaller band gap can lead to the creation of a degenerate electron gas at the heterojunction interface. The most widely used example of this technique is the GaAs-AlGaAs system, where the tertiary alloy is characterised by the fraction of aluminum atoms, i.e. $Al_xGa_{(1-x)}As$, with typically $x \simeq 0.3$.

| Material | $Al_xGa_{(1-x)}As$ | $GaAs$ |
|---|---|---|
| - | n-doped (Si) $10^{18}$ cm$^{-3}$ | p-type, weak or undoped, $10^{15}$ cm$^{-3}$ |
| Band gap | $E_g \simeq 1.42$ - 2.16 eV | $E_g \simeq 1.42$ eV |

This combination yields the "self-consistent" conductance band structure shown in Figure 2.29. It thus leads to the creation of a roughly triangular quantum well at the heterojunction interface. By careful tuning of the energies involved, one can engineer the band structure such that only the first discrete energy level within the quantum well lies below the Fermi energy. At low temperatures, only states in the first energy level $E_1$ are occupied and a **two-dimensional electron gas** is created.
In order to get some insight into the details of this configuration, the thermodynamic problem taking into account both the electrostatics (Poisson equation) and the quantum mechanics (Schrödinger equation) of the triangular potential well can be solved. For a triangular quantum well, the lowest quantised state can be related to the field

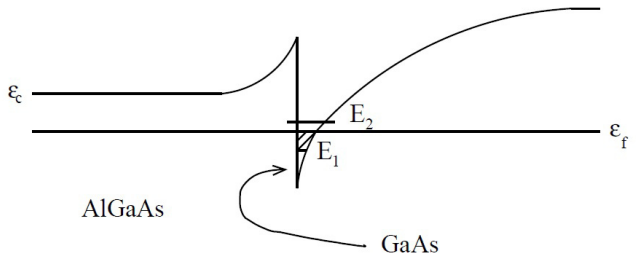


Fig. 2.29: Creation of a triangular quantum well in an AlGaAs-GaAs heterostructure

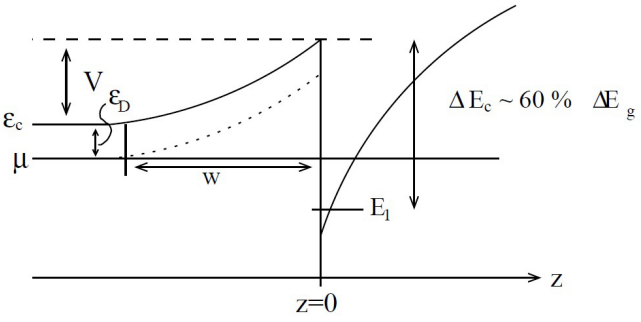


Fig. 2.30: Relevant parameters of the approximately triangular potential well

strength $F$ at the interface via

$$E_1 = \left(\frac{\hbar^2}{2m^*}\right)^{1/3}\left(\frac{9\pi eF}{8}\right)^{2/3} \tag{2.51}$$

(cf. chapter Field Effect Transistor), and hence via Gauss to the surface density of electrons $N_S$ at, or rather in the vicinity of, the interface where the band bending occurs. The relevant parameters are indicated in Fig. 2.30.

$$F = \frac{N_S e}{\epsilon_0 \epsilon_r} \tag{2.52}$$

Inserting $F$, the lowest energy state can directly be related to the 2D density $N_S$:

$$E_1 = \left(\frac{\hbar^2}{2m^*}\right)^{1/3}\left(\frac{9\pi e^2 N_S}{8\epsilon_0 \epsilon_r}\right)^{2/3} = const. * N_S^{2/3} \tag{2.53}$$

For a two-dimensional system the density is also implicitly related to the Fermi energy and wave vector, thus:

$$E_F = E_1 + \frac{\hbar^2 k_F^2}{2m^*} = E_1 + \frac{\pi\hbar^2}{m^*} N_S \tag{2.54}$$

using $k_F^2 = 2\pi N_S(2D)(= k_x^2 + k_y^2)$; $\quad k_F^3 = 3\pi^2 N_V(3D)$.

Under the assumption of a constant dopant density $N_d$ in the AlGaAs material and the condition for charge neutrality $N_d w = N_S$ (assuming that the excess electrons of the

surface electron density $N_s$ result from redistributing electrons with the bulk density $N_d$ across the depletion length $w$ of the band bending region), we can calculate the depletion potential by integration:

$$V_{dep} = -\int_0^{-w} F dz = \int_0^{-w} \frac{eN_d z}{\epsilon_0 \epsilon_r} dz = \frac{eN_d w^2}{2\epsilon_0 \epsilon_r} \tag{2.55}$$

From the above, the band edge discontinuity $\Delta\epsilon_C$ can be calculated to

$$\Delta\epsilon_C = E_1(N_S) + \frac{\pi\hbar^2 N_S}{m^*} + \epsilon_D + eV_{dep} \tag{2.56}$$

with $\epsilon_D$ the energy spacing between the Fermi level and $\epsilon_C$. Once $\Delta\epsilon_C$ is determined, the above can be used as a method for computing the two-dimensional density:

$$\Delta\epsilon_C - \frac{e^2 N_S^2}{2\epsilon_r \epsilon_0 N_d} - \epsilon_D = E_1(N_S) + N_S \frac{\pi\hbar^2}{m^*} \tag{2.57}$$

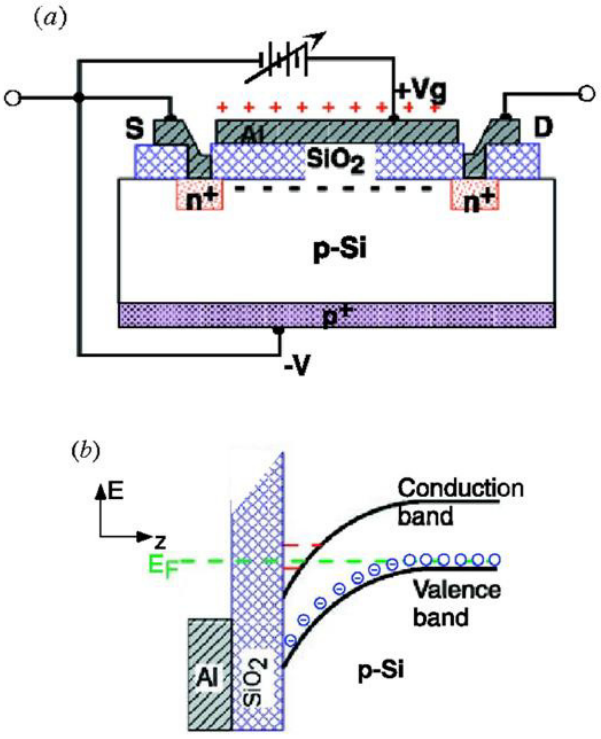


Fig. 2.31: Realization of a two-dimensional electron gas in a silicon MOSFET

Figure 2.31 schematically shows the realization of a two-dimensional electron gas in a Metal-Oxide-Seminconductor Field Effect Transistor (MOSFET). Figure 2.32 outlines the geometry of a GaAs/AlGaAs heterostructure including a two-dimensional electron gas. State-of-the-art two-dimensional electron gases in GaAs/AlGaAs at temperatures $< 1\,\mathrm{K}$ can exhibit ultra-high electron mobilities up to $> 10^7\ \mathrm{cm}^2/(\mathrm{Vs})$!

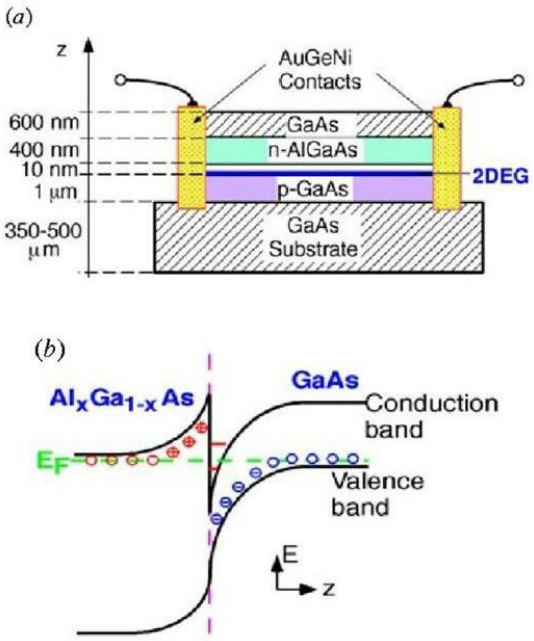


Fig. 2.32: Realization of a 2D electron gas in a GaAs/AlGaAs heterostructure

The experimental realisation of a GaAs/AlGaAs sample for low-temperature transport measurements is sketched in Figs. 2.33 and 2.34. The layer system is grown by molecular beam epitaxy with single atomic layer precision. A superlattice buffer of ultra-thin alternating GaAs and AlGaAs layers is grown to create an atomically flat surface on top of a GaAs substrate by making use of the strain induced by the slightly different lattice spacings. The 2D electron gas is created at the interface between the following GaAs and AlGaAs layers. A silicon doped AlGaAs layer is introduced to supply additional electrons to the 2D electron gas, but is separated from the interface by an undoped layer to reduce impurity scattering. The top layers are added to avoid oxidation. The conductance band edge corresponding to this layer structure is shown in Fig. 2.33 (left) and exhibits a triangular quantum well below the Fermi energy at the location of the 2D electron gas, where locally a high electron density is observed. Fig. 2.34 schematically outlines the steps for fabricating a sample with a buried 2D electron gas contacted by electrodes using optical lithography. A photoresist layer is spin-coated onto the GaAs/AlGaAs substrate with the buried 2D electron gas. The resist is structured through a mask by optical lithography, and a mesa structure is defined after wet-chemical development. The mesa structure is transferred into the substrate by etching until the 2D electron gas outside the mesa structure is removed. After removal of the residual resist, the final mesa structure is defined in the substrate. This Hall bar is contacted by repeating the optical lithography steps (second mask level) to define metallic contacts, which are annealed at several 100 °C to contact the buried electron gas with ohmic current-voltage-characteristics. The ohmic contacts are covered by larger metallic bond pads in the next optical lithography steps (third mask level) which are used for attaching thin metallic wires by wire bonding. The other side of the wires is attached to a chip carrier. By contacting the chip carrier, low currents can be applied to the structure, and the longitudinal and transversal voltages can be measured in a four-point configuration.

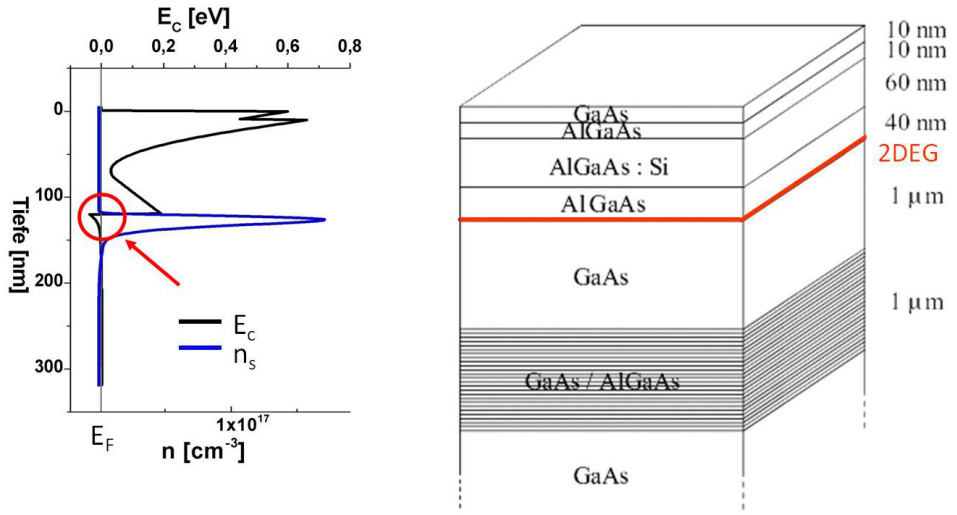


Fig. 2.33: Epitaxial layer system of a GaAs/AlGaAs sample with a 2D electron gas with corresponding conductance band structure $E_c$ and (quasi-)free electron density $n_s$

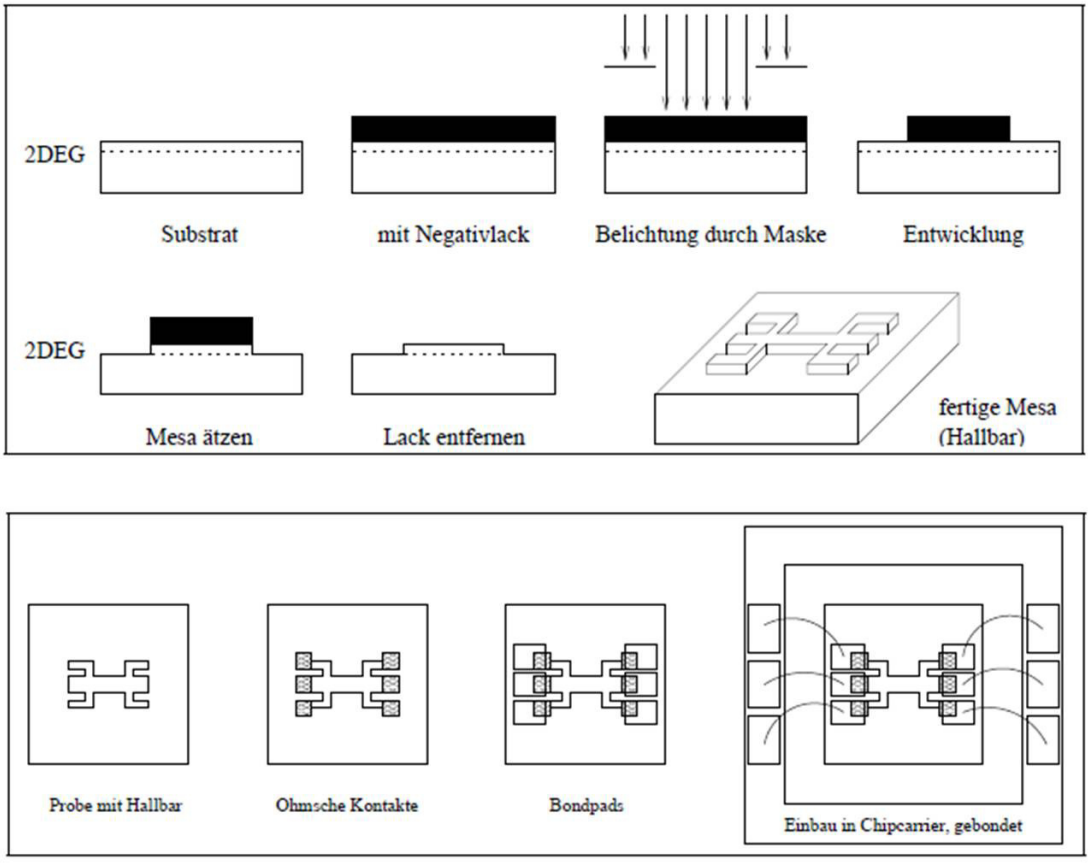


Fig. 2.34: Schematic fabrication steps of a “mesa” (Hall bar) structure for transport measurements in a 2D electron gas

### 2.4.2 Conductance in low-dimensional systems

The Boltzmann conductivity may be derived by considering the motion of an electron under the influence of an external force $\vec{f}(t)$ and the assumption of a relaxation time $\tau$ (mean time between collisions) in which the momentum of an electronic state is randomised. The electronic velocity $\vec{v}$, or equally the momentum $\vec{p}$, can readily be related to the current density $\vec{j}$ carried by an ensemble of such electrons in the material:

$$\vec{j} = -ne\vec{v} = -\frac{ne\vec{p}}{m^*} \tag{2.58}$$

where $n$ is the density of valence electrons and $m^*$ the effective mass. In the relaxation time approximation the evolution of the momentum as a function of time can be obtained by considering how such an electron evolves under the external field. Neglecting second order corrections, one gets a differential equation for the momentum $\vec{p}(t)$:

$$\frac{d\vec{p}}{dt} = -\frac{\vec{p}(t)}{\tau} + \vec{f}(t) \tag{2.59}$$

This expression can be applied to many cases of practical interest. Considering the simple case $\vec{f}(t) = -e\vec{E}$, the average momentum per carrier is expected to be independent of time, leading to

$$\frac{d\vec{p}}{dt} = -\frac{<\vec{p}>}{\tau} - e\vec{E} = 0 \tag{2.60}$$

Thus $<\vec{j}>= \frac{ne^2\tau}{m^*}\vec{E}$. This microscopic version of Ohm's law relates the local current density to the field strength, and the constant of proportionality $\sigma = \frac{ne^2\tau}{m^*}$ is called the **Boltzmann conductivity**. In general the effective mass $m^*$ is a tensor, $\frac{1}{M_{ij}} = \frac{1}{\hbar^2}\frac{\partial^2\epsilon}{\partial k_i \partial k_j}$, i.e. $\vec{j}$ is not necessarily parallel to $\vec{E}$, but for isotropic crystal systems the effective mass may be taken as a scalar quantity.

The mean free time is determined by temperature-dependent scattering mechanisms. At low temperatures, few phonons are available for scattering, and impurity scattering becomes dominant.

**Role of the electrons at the Fermi surface:**

In a simple picture, the Fermi surface under the influence of an external field can be considered as a shifted Fermi surface in k-space, which constantly relaxes to the ground state as a result of scattering (Fig. 2.35).

For sufficiently low field strengths, the electronic transport can be regarded as a property of the electrons at the Fermi surface. With $\Delta k \ll k_F$ or $\frac{\Delta k}{k_F} \ll 1$

$$\frac{\Delta\vec{p}}{\hbar k_F} \ll 1 \quad \text{or} \quad \frac{eE\tau}{\hbar k_F} \ll 1 \quad \Rightarrow \quad E < 10^5\,\mathrm{Vm}^{-1} \tag{2.61}$$

In low temperature experiments one generally considers **linear response properties** (limit $E \to 0$), thus the perturbations of the Fermi surface are minimal (typical experiments: 10 $\mu$V applied to 1 mm devices $\hat{=}$ $10^{-2}$ $\mathrm{Vm}^{-1}$).

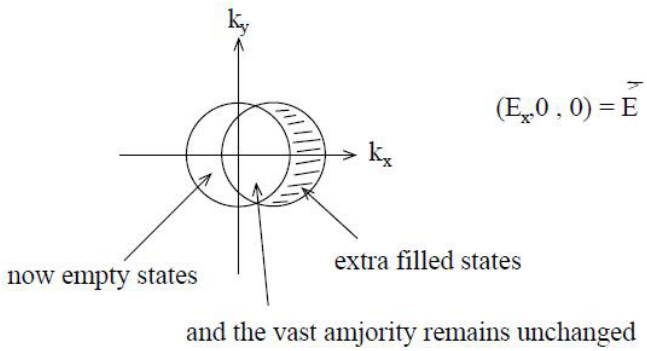


Fig. 2.35: Shift of the Fermi surface in an external field

For free electrons, $\epsilon_F = \frac{\hbar^2 k_F^2}{2m}$, and the electron density can be written as $n = \frac{k_F^d}{d(\pi^{d-1})}$, with $d$ the dimensionality of the system and $d \in \{2, 3\}$. The density of states then is

$$g(\epsilon_F) = \frac{dn}{d\epsilon}|_{\epsilon=\epsilon_F} = \frac{2m(2m\epsilon)^{\frac{d}{2}-1}}{\hbar^d \cdot 2(\pi^{d-1})} \tag{2.62}$$

With some simple manipulations the Boltzmann conductivity can be rewritten as

$$\sigma_B = \frac{ne^2\tau}{m} = g(\epsilon_F)e^2 \cdot \frac{2\epsilon_F\tau}{md} \tag{2.63}$$

The factor $\frac{2\epsilon_F\tau}{md}$ is known as the **Einstein diffusion constant**:

$$D = \frac{2\epsilon_F\tau}{md} = \frac{v_F^2\tau}{d} \tag{2.64}$$

with the Fermi velocity $v_F = \hbar k_F/m$. This approach to electronic transport demonstrates that the conductivity may be related purely to the electrons at the Fermi surface and the diffusion constant for their motion: $\boxed{\sigma_B = g(\epsilon_F)e^2D}$ + quantum corrections.

### Mesoscopic length scales

The **mesoscopic regime** addresses the intermediate transition region between the classical and the quantum mechanical regime, typically on a length scale of $\sim 1\,\mu$m to 100 nm, where objects start revealing quantum mechanical properties.

The **quantum corrections** observed in mesoscopic samples depend strongly on the interplay of many different length scales. In the low-temperature limit inelastic scattering mechanisms become weaker, and the dominant scattering mechanism is elastic scattering from fixed impurities (e.g. dopant atoms). The associated scattering time determines many parameters and different transport regimes.

**Relevant length scales** include:

- **Fermi wavelength** $\lambda_F = \frac{2\pi}{k_F}$ : largely independent of dimensionality, relatively large in semiconductor systems

- **Eleastic mean free path $l_e$:** also known as elastic scattering or momentum relaxation length; $l_e = v_F \tau_e$ with $v_F = \frac{1}{\hbar}(\frac{\partial \epsilon}{\partial k})_{k=k_F}$, $\tau_e$ elastic scattering time
- **Inelastic scattering length $l_{in} = \sqrt{D\tau_{in}}$:** generally associated with energy relaxation and therefore phase-relaxation of the eletronic wave functions
- **Phase coherence length $l_\Phi$:** Often, but not always equal to the inelastic scattering length
- **Magnetic length $l_B = \sqrt{\frac{\hbar}{eB}}$:** a phase shift of the wave functions leads to modified interference (Aharonov Bohm effect) or a loss of coherence (weak localisation)
- **Sample size $L_x, L_y, L_z$:** Plays a crucial role in determining both the dimensionality of the density of states and the dimensionality of the observed phenomena.

### Low-dimensional systems

By introducing **geometric restrictions**, the motion of charge carriers can be constrained in one or more dimensions through growth techniques and/or surface properties, as well as lateral structuring by electron beam lithography. The density of states is modified. By performing low-temperature measurements, it is possible to only populate the lowest available states in k-space in any given dimension(s).
As a consequence, a **2-dimensional electron gas** can be created. Quantisation into **Landau levels** appears when sufficiently high magnetic fields are applied, leading to the appearance of the **Quantum Hall Effect** in 2-dimensional systems. In **(quasi-)1-dimensional quantum wires or quantum point contacts**, **conductance quantisation** is observed in the transport properties of the wire. In **(quasi-)0-dimensional quantum dots**, their discrete energy level systems lead to **Coulomb blockade** and the observation of **charge quantisation** in the transport.
In the following the different quantisation mechanisms will be examined more closely.